

# Effective connectivity and neuroimaging

Christian Büchel and Karl J. Friston

## Contents

- I. Introduction**
- II. Origins and definitions**
- III. The basic linear model**
- IV. Nonlinear effective connectivity between V1 and V2**
- V. Structural equation modelling**
- VI. An example: Changes of effective connectivity**
- VII. Regression with time varying coefficients**
- VIII. Issues of validity**

## I. Introduction

In the past decade functional neuroimaging has been extremely successful in establishing functional segregation as a principle of organisation in the human brain. Functional segregation is usually inferred by the presence of activation foci in change or statistical parametric maps. The nature of the functional specialisation is then attributed to the sensorimotor or cognitive process that has been manipulated experimentally. Newer approaches have addressed the integration of functionally specialised areas through characterising neurophysiological activations in terms of distributed changes (e.g. McIntosh et al 1994a, Friston et al 1993a, Friston et al 1993b, Lagreze et al 1993, McIntosh & Gonzalez-Lima 1991, Horwitz *et al.*, 1995; Horwitz and Sporns, 1994). These approaches have introduced a number of concepts into neuroimaging (e.g. functional and effective connectivity, eigenimages, spatial modes, information theory, multidimensional scaling) and their application to issues in imaging neuroscience (e.g. functional systems, cortical integration, associative plasticity, and nonlinear cortical interactions). The study of effective connectivity will also gain importance for relating cognitive theories (eg. attention) to brain operations. For example categorical comparisons of functional brain imaging data suggests modulation of extrastriate cortical responses by attentional processes (Corbetta et al 1991). It would be very compelling to demonstrate the modulation of responsiveness of these areas in terms of attention-dependent changes in the interactions or effective connectivity among.

The aim of this chapter is to review some key applications of effective connectivity in terms of functional imaging using positron emission tomography (PET) and functional magnetic resonance imaging (fMRI). In neuroimaging functional connectivity is defined as the temporal correlations between remote neurophysiological events, whereas effective connectivity is defined as the influence one neural system exerts over another. Functional connectivity is simply a statement about the observed correlations; it does not provide any direct insight into how these correlations are mediated. For example, at the level of multiunit micro-electrode recordings, correlations can result from *stimulus-locked transients*, evoked by a common afferent input, or

reflect *stimulus-induced oscillations* - phasic coupling of neural assemblies, mediated by synaptic connections (Gerstein et al 1989). To clarify this distinction let us consider a simple example:

The mediodorsal nucleus of the thalamus is interconnected with different cortical areas. Increased activity in this structure will therefore lead to highly correlated brain activity in the cortical terminal fields of its projections, despite the fact that the cortical areas may not be directly connected. Eigenimage analysis (i.e. functional connectivity) of the cortical data, without the thalamus, would reveal a functional network of cortical areas. This example highlights the teleological weakness of functional connectivity and speaks to the importance of directly modelling interactions using effective connectivity.

We will introduce effective connectivity and consider some of the validation issues that ensue. Some of the more powerful applications of effective connectivity are concerned with *changes* in effective connectivity (e.g. time-dependent changes during procedural learning). Such an application is illustrated by characterising nonlinear interactions between striate (V1) and extrastriate (V2) cortices using fMRI data from a single-subject photic stimulation study. This modulatory interaction between V2 and V1 serves as an example of *activity-dependent* change in effective connectivity.

One method used to estimate effective connectivity is the application of structural equation modelling to functional brain imaging data. This technique combines an *anatomical* (constraining) *model* and the interregional covariances of activity. The ensuing *functional model* represents the influence of regions on each other through the putative anatomical connections. These influences can be either direct or indirect. Changes in effective connectivity in the dorsal visual stream (Mishkin *et al.*, 1983) due to attention serve as an example to illustrate this technique. This chapter will conclude with a critique of the proposed models of effective connectivity.

## II. Origins and definitions

The concept of effective connectivity was originated in the analysis of separable spike trains obtained from multiunit electrode recordings (e.g. Gerstein and Perkel 1969, Gerstein *et al* 1989; Gochin *et al* 1991; Aertsen and Preissl 1991).

Effective connectivity is closer to the intuitive notion of a connection than functional connectivity and can be defined as *the influence one neural system exerts over another* (Friston *et al* 1993b), either at a synaptic (c.f. synaptic efficacy) or cortical level. In electrophysiology there is a close relationship between effective connectivity and synaptic efficacy; "It is useful to describe the effective connectivity with a connectivity matrix of effective synaptic weights. Matrix elements  $[C_{ij}]$  would represent the effective influence by neuron  $j$  on neuron  $i$ " (Gerstein *et al* 1989). It has also been proposed that "the [electrophysiological] notion of effective connectivity should be understood as the experiment and time-dependent, simplest possible circuit diagram that would replicate the observed timing relationships between the recorded neurons" (Aertsen & Preissl 1991).

Although functional and effective connectivity can be invoked at a conceptual level in both neuroimaging and electrophysiology they differ fundamentally at a practical level. This is because the time-scales and nature of the neurophysiological measurements are very different (seconds *vs.* milliseconds and hemodynamic *vs.* spike trains). In electrophysiology it is often necessary to remove the confounding effects of stimulus-locked transients (that introduce correlations *not* causally mediated by direct neural interactions) in order to reveal the underlying connectivity. The confounding effect of stimulus-evoked transients is less problematic in neuroimaging because the promulgation of dynamics from primary sensory areas onwards *is* mediated by neuronal connections (usually reciprocal and interconnecting). However it should be kept in mind that functional connectivity is not necessarily due to effective connectivity.

## III. The basic linear model

Functional connectivity is an operational definition. Effective connectivity is not; it depends on two models: a mathematical model, describing "how" areas are connected and a neuroanatomical model describing "which" areas are connected. We shall consider linear and nonlinear models. Perhaps the simplest model of effective connectivity expresses the hemodynamic change at one voxel as a weighted sum of changes elsewhere. The weights or coefficients can then be identified with effective connectivity: For example let the activity of voxel  $i$  be  $m_i$  then:

$$m_i = C_{ij}.m_j + e_i$$

or in matrix notation:  $\mathbf{m}_i = \mathbf{M}.C_i + \mathbf{e}$  1

where  $C_i$  is a column-vector of effective connection estimates from all locations to the one in question ( $i$ ).  $\mathbf{e}$  is an error term. If one selects a point ( $i$ ) in the brain and asks; what is the effective connection strength between the location chosen and all other locations? Then one wants to know the values of  $C_i$ . The least squares solution for  $C_i$  is (Binmore 1982):

$$C_i = (\mathbf{M}^T.\mathbf{M})^{-1}.\mathbf{M}^T.\mathbf{m}_i$$
 2

This solution can be regarded as a linear regression, where the effective connectivity reflects the amount of rCBF variability, at  $i$ , attributable to rCBF changes at location  $j$ . Implicit in this interpretation is a mediation of this influence by neuronal connections with an effective strength equal to  $C_{ij}$ . There are many issues that deserve comment when estimating effective connectivity in this way. First the fact that there are only a few observations (e.g. 12 in the PET study of the previous chapter) but many (e.g. 6477) voxels means the above equations are very under-determined. This problem is dealt with finding a solution with the minimum 2-norm (Golub and Van Loan 1991). This in turn is equivalent to solving the equation in the space defined by the eigenimages (see the previous chapter). Mathematically:

$$\mathbf{m}_i = \mathbf{M}.\mathbf{v}.\mathbf{a}_i + \mathbf{e}$$
 3

is solved for  $\mathbf{a}_i$ , where  $C_i = \mathbf{v}.\mathbf{a}_i$ . As in the previous chapter  $\mathbf{v} = [\mathbf{v}^1 \dots \mathbf{v}^r]$  is a matrix of  $r$  eigenimages and  $\mathbf{M}.\mathbf{v} = \mathbf{u}.\mathbf{s}$ . Only the  $r$  (or less) eigenvectors with non-zero (or large) eigenvalues are used, giving:

$$C_i = \mathbf{v} \cdot \mathbf{s}^{-2} \cdot \mathbf{v}^T \mathbf{M}^T \cdot \mathbf{m}_i = \mathbf{v} \cdot \text{pinv}(\mathbf{M} \cdot \mathbf{v}) \cdot \mathbf{m}_i \quad 4$$

$\text{pinv}(\cdot)$  denote the pseudo inverse. Provisional experience suggests that the linear model [Eq. (1)] can be well behaved. One explanation is that the dimensionality (the number of things which are going on) of the physiological changes can be small. In fact the distribution of eigenvalues associated with the PET study of the previous chapter suggested a dimensionality of two. In other words the brain responds to simple and well organized experiments in a simple and well organized way. In the PET example, despite having measurements in 6477 voxels there were only substantial changes in two eigenimages.

Generally however neurophysiology is nonlinear and the adequacy of linear models must be questioned (or at least qualified). Consequently we focus on a nonlinear model of effective connectivity that is an extension of the linear framework presented in this section. This model was designed to answer a specific but important question about modulatory interactions in visual cortex:

## IV. Nonlinear effective connectivity between V1 and V2

### IV.A. Modulatory interaction in visual cortex

Reversible cooling experiments in monkey visual cortex, during visual stimulation, have demonstrated that neuronal activity in V2 depends on forward inputs from V1. Conversely neuronal activity in V1 is *modulated* by backward or reentrant connections from V2 to V1 (Schiller & Malpeli 1977, Sandell & Schiller 1982, Girard & Bullier 1988). Evidence for these functional asymmetries is found in the work of Schiller and colleagues (Schiller & Malpeli 1977, Sandell & Schiller 1982). Retinotopically corresponding regions of V1 and V2 are reciprocally connected in the monkey. V1 provides a crucial input to V2, in the sense that visual activation of V2 cells depends on input from V1. This dependency has been demonstrated by reversibly cooling (deactivating) V1 while recording from V2 during visual stimulation (Schiller & Malpeli 1977, Girard & Bullier 1988). In contrast, cooling V2 has a more *modulatory* effect on V1 unit activity. "Most cells became less responsive to visual stimulation, while a few became more active during cooling". The cells in V1 that were most affected by V2 deactivation were in the infragranular layers, suggesting V2 may use this pathway to modulate the output from V1 (Sandell & Schiller 1982). Similar conclusions about the return pathway between V5 and V2 were drawn by Girard and Bullier (1988): Because, in the absence of V1 input, these reentrant connections do not constitute an efficient drive to V2 cells, their role is most likely "to modulate the information relayed through area 17" (V1).

### IV.B. A nonlinear model of effective connectivity

To examine the interactions between V1 and V2, using fMRI in man, we have used a nonlinear model of effective connectivity, extended to include a modulatory interaction [c.f. Eq (1)]:

$$m_i = (C^{O_{ij}} \cdot m_j + C^{M_{ij}} \cdot m_j m_i) \quad 5$$

This model has two terms that allow for the activity in area  $i$  to be influenced by the activity in area  $j$ . The first represents an effect which depends only on afferent input from area  $j$ . This is the activity in  $j$  scaled by  $C^{O_{ij}}$ . The coefficient  $C^{O_{ij}}$  is referred to as an *obligatory* connection strength, in the sense that a change in area  $j$  results in an obligatory response in area  $i$ . Conversely the second term reflects a modulatory influence of area  $j$  on area  $i$ . The coefficient determining the size of this effect ( $C^{M_{ij}}$ ) is referred to as a *modulatory* connection strength, because the overall effect depends on both the afferent input ( $C^{M_{ij}} \cdot m_j$ ) and intrinsic activity ( $m_i$ ).

This equation, or model, can be interpreted from two points of view; (i) by analogy with the nonlinear behaviour that characterizes voltage-dependent channels in electrophysiology or (ii) in terms of classical (pharmacological) neuromodulation where post-synaptic responsiveness is modulated without a direct effect on post-synaptic membrane potential. The voltage-dependent analogy is obtained by considering  $m_i$  as post-synaptic potential and  $m_j$  as a depolarizing current. According to Eq(5) a high  $C^{M_{ij}}$  reflects *a greater sensitivity to changes in input at higher levels of intrinsic activity*. In electrophysiological terms this translates as a change in post-synaptic depolarization, in response to a fixed depolarizing current, which increases with depolarization: This is a characteristic of voltage-dependent interactions (Haberly 1991). This intrinsic activity-dependent effect, determined by the value of  $C^{M_{ij}}$ , provides an intuitive sense of how to estimate  $C^{M_{ij}}$ . This estimation involves

measuring the difference in sensitivity between states with high and low intrinsic activity at the location of interest:

Imagine one were able to 'fix' the activity in V1 at a low level and measure the connectivity between V2 and V1 assuming a simple linear relationship [Eq. (1)]: A value for the sensitivity of V1 to V2 changes could be obtained, say C1. Now, if the procedure were repeated with V1 activity fixed at a high level, a second (linear) estimate would be obtained (C2). In the presence of a substantial modulatory interaction between V2 and V1 the second estimate will be higher than the first. This is because the activity intrinsic to V1 is higher and V1 should be more sensitive to inputs from V2. In short C2 - C1 provides an estimate of the modulatory influence of V2 on V1. The activity of V1 can be fixed *post hoc* by simply selecting a subset of data in which the V1 activity is confined to some small range.

An estimation of the effective connection strengths of both an obligatory and modulatory nature can be obtained for the connections between *all* voxels and a reference location in the following way; for any reference location (*i*) assume that a subset of the time-series can be selected so that  $m_i$  is limited to some small range about its mean ( $\langle m_i \rangle$ ). For this subset Eq. (5) can be approximated by Eq. (1) (omitting error terms for clarity):

$$m_i = C^{O_{ij}.m_j} + \langle m_i \rangle C^{M_{ij}.m_j} \\ m_j \cdot (C^O + \langle m_i \rangle C^M) \\ m_j \cdot C \quad 6$$

Where  $C = C^O + \langle m_i \rangle C^M$ . Now assume two such subsets are selected, one with a high mean ( $\langle m_i \rangle_2$ ) and one with a low mean ( $\langle m_i \rangle_1$ ) giving two solutions for C ( $C_2$  and  $C_1$ ), then:

$$C^M = (C_2 - C_1) / (\langle m_i \rangle_2 - \langle m_i \rangle_1) \quad 7$$

(a similar expression for  $C^O$  can be derived - see Friston et al 1995). Again the estimate of ( $C_2 - C_1$ ) is computed in the space defined by the spatial modes in the same way as Eq. (4)

$$(C_2 - C_1) = v \cdot (\text{pinv}(M_2 \cdot v) \cdot m_{2i} - \text{pinv}(M_1 \cdot v) \cdot m_{1i}) \quad 8$$

where the subscripts 1 and 2 denote subsets of the time-series selected on the basis of intrinsic activity ( $m_i$ ) being low or high. This general approach to characterizing nonlinear systems with a piece-wise series of locally linear models has proved a fruitful strategy in many instances (Tsonis 1992). See Palus et al (1991) for a conceptually related approach to multichannel EEG recordings.

The hypothesis that asymmetrical nonlinear V1 - V2 interactions would characterize cortical interactions in human visual cortex can be formulated in terms of  $C^{M_{ij}}$ . We predicted that *anatomically* (i) the modulatory component of effective connections to V1 would be regionally specific and include V2 and that *functionally* (ii) the forward modulatory influences from V1 to V2 would be smaller than the reciprocal influences.

The data used in this analysis were a time-series of 64 gradient-echo EPI coronal slices (5 mm thick, with 64 x 64 voxels 2.5 x 2.5 x 5 mm) through the calcarine sulcus and extrastriate areas. Images were obtained every 3 seconds from a normal male subject using a 4.0 T whole body system, fitted with a small (27 cm diameter) z-gradient coil (TE 25 ms, acquisition time 41 ms). Photoc stimulation (at 16 Hz) was provided by goggles fitted with 16 light emitting diodes. The stimulation was off for the first 10 scans (30 seconds), on for the second 10, off for the third, and so on. Images were reconstructed without phase correction. The data were interpolated to 128 x 128 voxels. Each interpolated voxel thus represented 1.25 x 1.25 x 5 mm of cerebral tissue. The first 4 scans were removed to eliminate magnetic saturation effects and the remainder were realigned. The result of this preprocessing was a mean corrected data matrix  $M$  with 60 rows (one for each scan) and 2160 columns (one for each voxel).

#### IV.C. Regional specificity of modulatory connections to V1

A reference voxel was chosen in V1, according to the atlas of Talairach and Tournoux (1988), and the effective connection strengths  $C^{M_{V1,j}}$  were estimated according to Eq. (7) allowing a map of  $C^{M_{V1,j}}$  (and  $C^{O_{V1,j}}$ ) to be constructed. This map provides a direct test of the hypothesis concerning the topography and regional specificity of modulatory influences on V1. The lower row in Figure 1 shows maps of  $C^{O_{V1,j}}$  and  $C^{M_{V1,j}}$  (for a reference

in V1 on the right) and reflect the degree to which the area exerts an obligatory (left) or modulatory (right) effect on V1 activity. These maps have been thresholded at 1.64 after normalization to a standard deviation of unity. This corresponds to an uncorrected threshold of  $p = 0.05$ .

The obligatory connections to the reference voxel derive mainly from V1 itself, both ipsilaterally and contralaterally with a small contribution from contiguous portions of V2. The effective connectivity from contralateral V1 should not be over-interpreted given that (i) the source of many afferents to V1 (the lateral geniculate nuclei) were not included in the field of view and that (ii) this finding can be more parsimoniously explained by 'common input' (c.f. discussion of functional connectivity due to common input in the introduction to this chapter). As predicted, and with remarkable regional specificity, the modulatory connections were most marked from ipsilateral V2, dorsal and ventral to the calcarine fissure [Brodmann's area 18 according to the atlas of Talairach and Tournoux (1988)] (note that 'common input' cannot explain interactions between V1 and V2 because the geniculate inputs are restricted to V1).

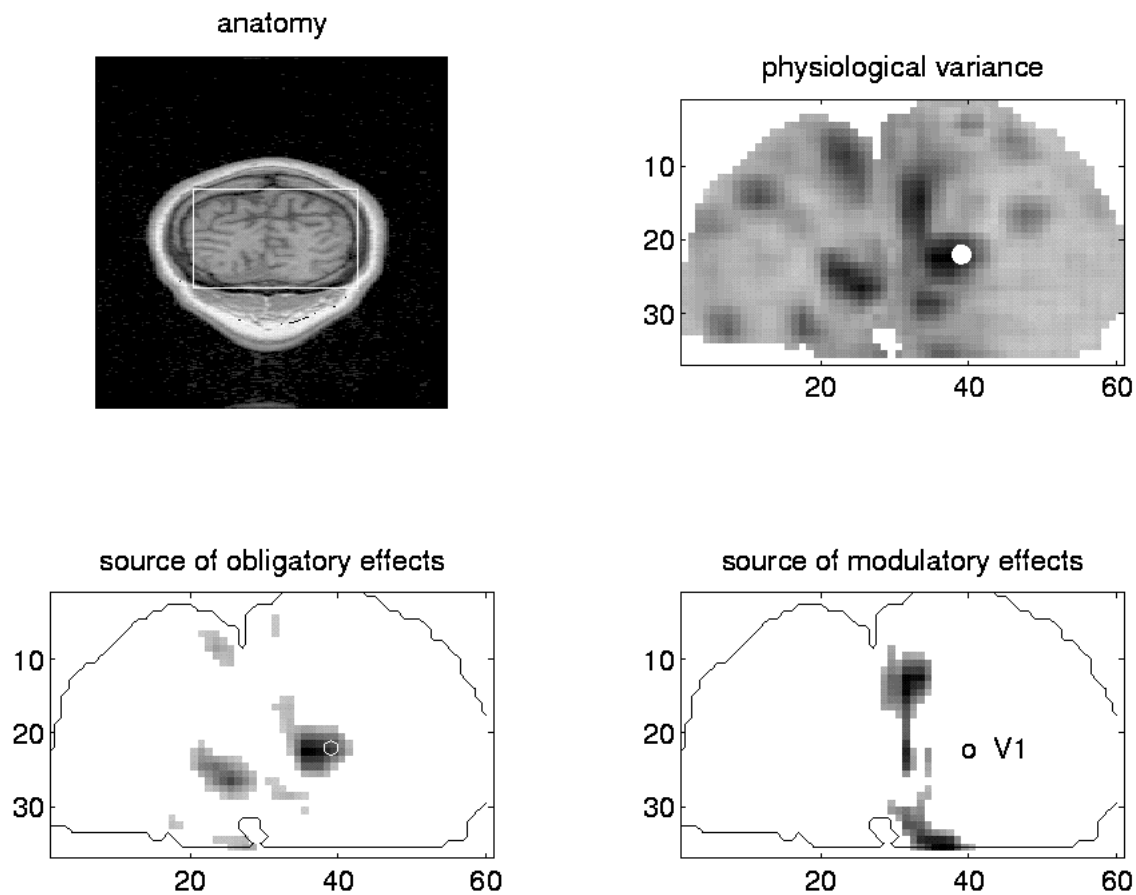


**Figure 1.** Maps of the estimates of obligatory and modulatory connection strengths to V1. Top left: Anatomical features of the coronal data used. This image is a high resolution anatomical MRI scan of the subject that corresponds to the fMRI slices. The box defines the position of a (36 x 60 voxel) subpartition of the fMRI time-series selected for analysis. Top right: The location of the reference voxel designated as V1 (white dot). This location is shown on a statistical parametric map of physiological variance (calculated for each voxel from the time-series of 60 scans). The image has been scaled to its maximum. Lower right and lower left: Maps of  $CO_{V1,j}$  and  $C^M_{V1,j}$ . The images have been scaled to unit variance and thresholded at  $p = 0.05$  (assuming, under the null hypothesis of no effective connectivity, the estimates have a Gaussian distribution). The reference voxel in V1 is depicted by a circle. The key thing to note is that V1 is subject to modulatory influences from ipsilateral and extensive regions of V2.

#### IV.D. Functional asymmetry in V2 - V1 and V1 - V2 modulatory connections

To address the functional asymmetry hypothesis the modulatory connection strengths between two extended regions (two 5 x 5 voxel squares) in ipsilateral V1 and V2 were examined. The estimates of effective connection strengths were based on hemodynamic changes in all areas and the subset of connections between the two regions were selected to compare the distributions of forward and backward modulatory influences. Figure 2 shows the location of the two regions (this time on the right) and the frequency distribution of the estimates for connections from the V1 box to the V2 box (broken line) and the corresponding estimates for connections from V2 to V1 (solid line). There is a remarkable dissociation, with backward modulatory effects (V2 to V1) being much greater than forward effects (V1 to V2). This can be considered a confirmation of the functional asymmetry hypothesis.

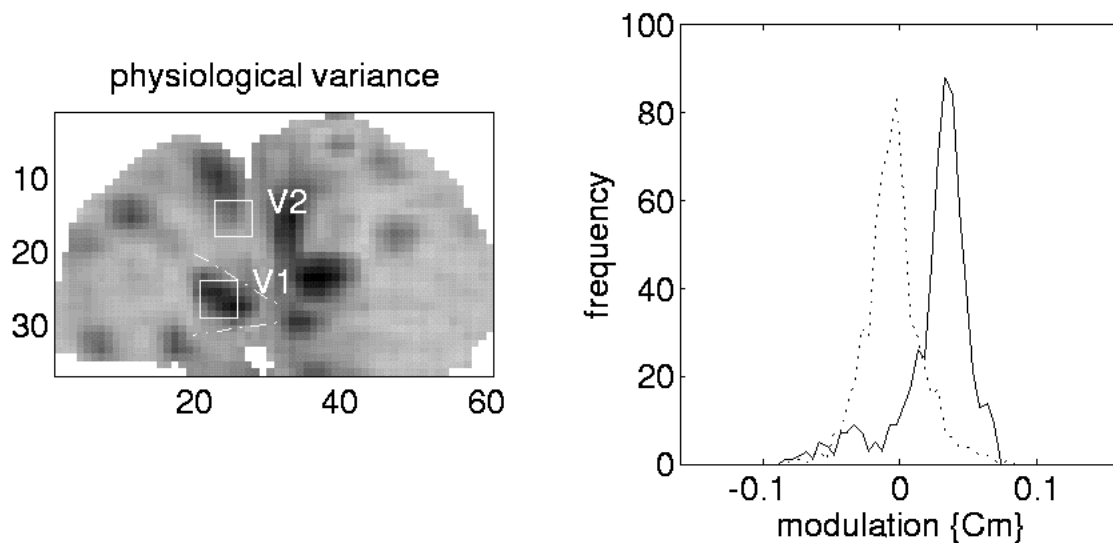


**Figure 2.** Graphical presentation of a direct test of the hypothesis concerning the asymmetry between forward and backward V1 - V2 interactions. Left: a map of physiological variance showing the positions of two boxes defining regions in V1 and V2. The broken lines correspond (roughly) to the position of the V1/V2 border according to the atlas of Talairach and Tournoux (1988). The value of  $CM_{ij}$  were computed for all voxels in either box and Euclidean normalized to unity over the image. The frequency distribution of  $CM_{ij}$  connecting the two regions is presented on the right. The backward connections (V2 to V1 - solid line) are clearly higher than the corresponding forward connections (V1 to V2 - broken line).

## V. Structural equation modelling

Structural equation modelling or path analysis is a technique developed in economics, psychology and the social sciences. The basic idea is different from the usual statistical approach of modelling individual observations. In multiple regression or Anova the regression coefficients or the error variance derive from the minimisation of the sum of squared differences of the predicted and observed dependent variables. Structural equation modelling approaches data from a different perspective: instead of considering variables individually, the emphasis lies on the variance-covariance structure. Thus models are solved in structural equation modelling by minimising the difference between the observed variance-covariance structure and the one implied by a structural or path model. In the past few years structural equation modelling has been applied to functional brain imaging. McIntosh and Gonzales-Lima (1994b) demonstrated the dissociation between ventral and dorsal visual pathways for object and spatial vision using structural equation modelling of PET data in the human. In this chapter we will focus on the theoretical background of structural equation modelling and demonstrate the adaptation of this

technique to functional brain imaging with a fMRI study. This study looked at the effect of attention to visual motion on effective connectivity in the dorsal visual stream.

In terms of neural systems a measure of covariance represents the degree to which the activities of two or more regions are related (i.e. functional connectivity). The study of variance-covariance structures in neurosciences has a major advantage compared to applications of this technique in other fields: the interconnection of the dependent variables (regional activity of brain areas) is anatomically determined and the activation of each region can be directly measured with functional brain imaging. This is a major difference to 'classical' structural equation modelling in the behavioural sciences, where models are highly hypothetical and contain latent variables, which represent a concept (e.g. intelligence) that cannot be measured directly.

### V.A Models

As mentioned above structural equation modelling minimises the difference between the observed  $\mathbf{S}$  and implied covariance matrix  $\hat{\mathbf{S}}$ . The variance-covariance structure  $\mathbf{S}$  of the observed variables is given by:

$$\mathbf{S} = \frac{1}{(N-1)} \mathbf{y}^T \mathbf{y} \quad 9$$

where  $\mathbf{y}$  is a  $N$  by  $p$  matrix of deviation (from the means) scores of the  $p$  observed variables with  $N$  observations and  $\mathbf{y}^T$  is  $\mathbf{y}$  transpose. The matrix  $\mathbf{S}$  is square and symmetric with the sample variances down its main diagonal and the covariances off the diagonal.

Consider a model, where variables  $\mathbf{x}$  are 'caused' by a set of independent variables  $\mathbf{z}$  (Figure 3). This could also be construed as a set of variables  $\mathbf{x}$  with residual influences  $\mathbf{z}$  (outside the model). In addition the variables  $\mathbf{x}$  may cause each other.

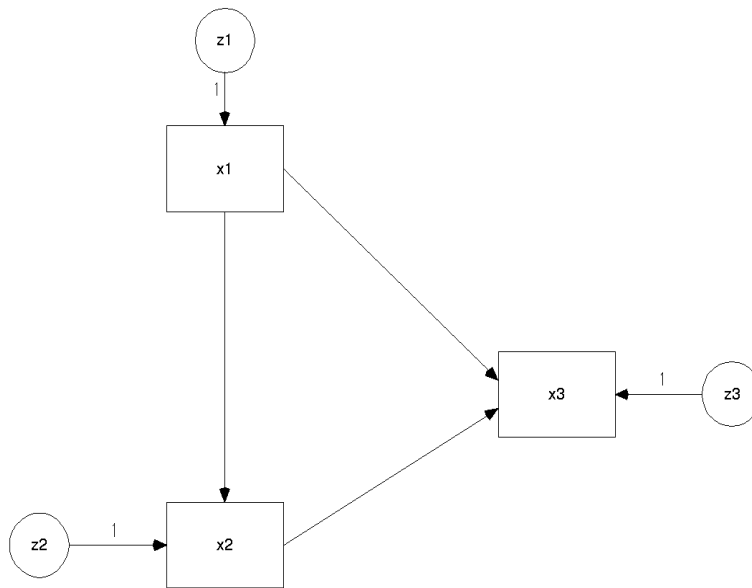


**Figure 3.** Simple path model to demonstrate the mathematical background of structural equation modelling.  $\mathbf{x}$  are observed variables, the (uni-directional) path coefficients between variables  $\mathbf{x}$  constitute matrix  $\mathbf{B}$ . The one at each path between  $\mathbf{z}$  and the corresponding variable  $\mathbf{x}$  denotes the fact that  $\mathbf{z}$  are residual variances, which are not explained by the model. The path-coefficients for the connections from  $\mathbf{z}$  to  $\mathbf{x}$  are therefore one, which is simply the identity matrix (see equation 10).

Algebraically, the model for  $\mathbf{x}$  is:

$$\mathbf{x} \cdot \mathbf{I} = \mathbf{x} \cdot \mathbf{B} + \mathbf{z} \quad 10$$

Where  $\mathbf{B}$  is a matrix of unidirectional path coefficients,  $\mathbf{I}$  is the identity matrix. Here  $\mathbf{x}$  appears on both sides of the equation. This reduces to

$$\mathbf{x} = \text{inv}(\mathbf{I} - \mathbf{B}) \cdot \mathbf{z} \quad 11$$

Looking at the variance-covariance structure and omitting the denominator  $(1/(N-1))$  we have:

$$\begin{aligned} \mathbf{x}^T \cdot \mathbf{x} &= (\text{inv}(\mathbf{I}-\mathbf{B}) \cdot \mathbf{z})^T \cdot (\text{inv}(\mathbf{I}-\mathbf{B}) \cdot \mathbf{z}) \\ &= \text{inv}(\mathbf{I}-\mathbf{B})^T \cdot \mathbf{C} \cdot (\text{inv}(\mathbf{I}-\mathbf{B})) \end{aligned} \quad 12$$

where  $\mathbf{C} = \mathbf{z}^T \cdot \mathbf{z}$

$\mathbf{B}$  is not symmetric because structural equation modelling allows asymmetric connections.  $\mathbf{C}$  is a diagonal matrix and contains the residual variances. If interaction between the residual influences were incorporated in the model, their covariances would appear (symmetrically) off the leading diagonal in  $\mathbf{C}$  (not shown in the Figure 3). This follows from the fact that  $\mathbf{C}$  is equal to  $\mathbf{z}^T \cdot \mathbf{z}$  which is the variance-covariance structure of  $\mathbf{z}$ . The denominator  $(1/N-1)$  is omitted for clarity. The solution of equation (12),  $\mathbf{x}^T \cdot \mathbf{x}$  is the implied variance-covariance structure. Parameters in  $\mathbf{C}$  and  $\mathbf{B}$ , which are to be estimated, are called free parameters. The free parameters are estimated by minimising a function of  $S$  and  $p$ . To date the most widely used objective function for structural equation modelling is the maximum likelihood (ML) function:

$$F_{ML} = -2 \log |S| + \text{tr}(S \cdot \text{inv}(\mathbf{C})) - \log |S| - p \quad 13$$

Where  $\text{tr}(\cdot)$  is the trace of the matrix and  $p$  is the number of free parameters. Starting values can be provided for the free parameters or estimated by a least squares approach (McIntosh et al., 1994a).

Numerical maximisation algorithms are employed to minimise (maximize) the maximum likelihood function. These algorithms either use the gradient of the ML function (e.g. steepest descent, Newton-Raphson) or employ a search in the parameter space (e.g. Nelder-Mead simplex search).

An important issue in structural equation modelling is the determination of the underlying anatomical model. Different objective methods can be combined: Categorical comparisons between different conditions, eigenimages highlighting structures of functional connectivity in conjunction with nonhuman electrophysiological and anatomical studies have been used (Grafton et al., 1994, McIntosh et al., 1994a). A model is always a simplification of reality: absolutely correct models either do not exist, or would be too complicated to understand. In the context of effective connectivity one has to find a compromise between complexity, anatomical accuracy and interpretability. There are also mathematical constraints on the model: if the number of free parameters (unknowns) exceeds the number of observed covariances the system is underdetermined and no single solution exists.

Statistical inference in structural equation modelling can address two points. The goodness of the overall fit of the model, i.e. how significantly different is the implied from the observed variance-covariance structure and the difference between different models (e.g. object versus spatial vision [McIntosh et al., 1994]). In the context of multivariate normally distributed variables the minimum of the maximum likelihood fit function times the number of observations minus one, follows a chi-square distribution with  $(q/2) \cdot (q+1) - p$  degrees of freedom (Bollen 1989).  $p$  is the number of free parameters and  $q$  is the number of observed variables. The hypothesis is that the model is not able to reproduce the observed variance covariance structure. That implies that a non-significant chi-square value is desired, if one wants to infer the validity of the hypothesis of no difference between model and data. This is problematic because, from the point of view of the  $\chi^2$ -statistic this is like trying to confirm the null hypothesis (of no differences). Generally one cannot confirm the null hypothesis: for example as the  $\chi^2$  value is a function of sample size, the rejection of the null hypothesis in small samples is very likely, but not necessarily due to a good model (but due to low power). In contrast to 'classical' path analysis, the validation of models used in the context of functional brain imaging relies on the neuroanatomy. Therefore goodness of fit estimation only plays a minor role. However, the goodness of fit measure might be useful, when comparing different models with each other. This so called 'stacked model' approach can be used to compare different models (e.g. data from different groups or conditions) in the context of structural equation modelling. A so called 'null-model' is constructed where the estimates of all free parameters are constrained to be the same for both groups. The alternative model allows the free parameters to differ between groups. The significance of the differences between the models is expressed by the difference of the chi-square goodness of fit indicator.

How are path coefficients interpreted? The path coefficients calculated by the minimisation procedure outlined above depend upon the units in which the variables are measured. Although all variables in functional imaging procedures are measured in the same units, the direct comparison of path coefficients between two different groups might be misleading due to different scaling (eg. global blood flow in PET). In this case standardised path coefficients are calculated. This is the path coefficient times the ratio of the standard deviations of the two connected variables (the standard deviation of the caused variable constituting the denominator). The standardised coefficient shows the mean response in units of standard deviation of the dependent variable for a standard deviation change in an explanatory variable, whilst the other variables in the model are held constant (Bollen 1989).

A major limitation of current applications of structural equation modelling is the restriction to linear models. This limitation can be overcome by introducing additional variables containing a non-linear function (e.g.  $f(x)=x^2$ ) of the original variables (Kenny and Judd, 1984). Interactions of variables can be incorporated in a similar fashion; wherein a new variable, containing the product of the two interacting variables, is introduced as an additional influence. The latter approach will be used to explain changes in effective connectivity in the dorsal visual stream by a moderator variable.

## **VI. An example: Changes of effective connectivity in the dorsal visual stream**

Electrophysiological and neuroimaging studies have shown that attention to visual motion can increase the responsiveness of the motion-selective cortical area V5 (O'Craven and Savoy, 1995, Treue and Maunsell, 1996) and the posterior parietal cortex (PP)(Assad and Maunsell, 1995). Increased or decreased activation in a cortical area is often attributed to attentional modulation of the cortical projections to that area. This leads to the notion that attention is associated with changes in connectivity.

Here we present fMRI data from an individual subject, scanned under identical visual motion stimulus conditions, changing only the attentional component of the tasks employed.

In the first stage we identified regions that show differential activations in relation to attentional set. In the second stage changes in effective connectivity between these areas are assessed using structural equation modelling. In the final stage we show how these attention dependent changes in effective connectivity might be explained by the modulatory influence of frontal cortical areas using a non-linear extension of structural equation modelling.

The experiment was performed on a 2 Tesla whole body MRI system equipped with a head volume coil. Contiguous multislice T2\* weighted fMRI images (TE=40ms; 90 ms/image; 64x64 pixels [19.2 cm x 19.2 cm]) were obtained with echo-planar imaging (EPI) using an axial slice orientation. A T2\* weighted sequence was chosen to enhance blood oxygenation level dependent (BOLD) contrast. The effective repetition time was 3.22 seconds.

The subject was scanned during 3 different conditions: “fixation”, “attention” and “no attention”. Each condition lasted 32.2 seconds giving 10 multislice volumes per condition. We acquired a total of 260 images.

During all conditions the subjects looked at a fixation point in the middle of a transparent screen. In conditions with visual motion (“attention” and “no attention”) 250 white dots (size 0.1°) moved radially from the fixation point in random directions towards the border of the screen, at a constant speed of 4.7° per second. The difference between “attention” and “no attention” lay in the explicit command given to the subject shortly before the condition: “just look” indicated “no attention” and “detect changes” the “attention” condition. Both visual motion conditions were interleaved with “fixation”. No response was necessary.

Before scanning, subjects were exposed to five 30 second trials of the stimulus. The speed of the moving dots was changed 5 times during each trial. Subjects were asked to indicate any change in speed. Changes in speed were gradually reduced over the 5 trials, until a 1% change was presented on the last occasion. Once in the scanner, changes in speed were completely eliminated (without the knowledge of the subject), so that identical visual stimuli were shown in all motion conditions.

Regions of interest were defined by categorical comparisons using the SPM{Z} comparing “attention” and “no attention” and comparing “no attention” and “fixation”. As predicted with a stimulus consisting of radially moving dots we found activation of primary visual cortex (V1), V5 and the posterior parietal complex. For the subsequent analysis of effective connectivity, we defined regions of interest (ROI) with a diameter of 8 mm, centred around the most significant ( $p<0.05$ , corrected) voxel as revealed by the categorical comparison. A single time-series, representative of this region, was defined by the first eigenvector of all the voxels in the ROI.

### *VI.A. Linear model of the dorsal visual stream for “attention” and “no attention”*

Our model included the LGN, primary visual cortex (V1), V5 and the posterior parietal complex (PP). Although connections between regions are generally reciprocal, due to mathematical restrictions (the relative numbers of known and unknown variables and stability of the model) we only included unidirectional paths.

To assess effective connectivity in a condition-specific fashion, we used time-series that comprised observations during the condition in question. Path coefficients for both conditions (“attention” and “no attention”) were estimated using a maximum likelihood function with the software package AMOS (Amos for Windows, Version 3.5, SmallWaters Corp., Chicago). To test for the impact of changes in effective connectivity between “attention” and “no attention”, we defined a free model (allowing for different path coefficients between V5 and PP for attention and no attention) and a constrained model (constraining the V5 -> PP coefficient to be equal).

This analysis revealed a highly significant difference ( $\chi^2=26, p<0.01$ ) in model fit in favour of the free model, indicating a significant change (ie. increase) in effective connectivity for “attention” (Figure 4).

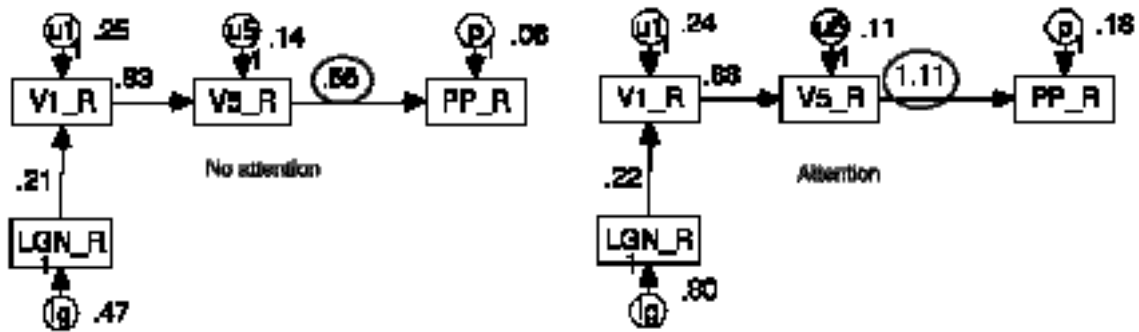


**Figure 4.** Structural equation model for the dorsal visual pathway. The parameters are evaluated for “attention” and “no attention” separately. It can be seen that the connectivity between V5 and PP is significantly larger during “attention” than during “no attention”.

### VI.B. Modelling modulation by interaction terms

The linear path model of the previous section comparing “attention” and “no attention” revealed increased effective connectivity in the dorsal visual pathway in relation to attention. The question that arises is which part of the brain is capable of modulating this pathway? Based on lesion studies (Lawler and Cowey, 1987) and on the system for directed attention as described by Mesulam (1990), the dorsolateral prefrontal cortex or the anterior cingulate were candidates for such a modulatory role (only the right dorsolateral prefrontal cortex showed a significant activation during “attention” relative to “no attention”).

The right prefrontal region was included in our model as a moderator variable modulating the posterior visual pathway. Given the neuroanatomical projection from PFC to PP, we included a modulation of the pathway between V5 and PP. Assuming a non-linear modulation of this connection, we constructed a new variable “V5PFC” in our analysis. This variable, mediating the interaction, is simply the time-series of region V5 multiplied by the time-series of the right prefrontal cortex. Although the time series are normalised before multiplication, the product of 2 variables (say V5 and PFC) will still show some correlation with the individual terms. Therefore we residualised the interaction term (V5 x PFC) by least squares:

$$V5 \times PFC = [V5 \ PFC] \cdot b + V5PFC$$

i.e.

$$V5PFC = V5 \times PFC - [V5 \ PFC] \cdot \text{pinv}([V5 \ PFC]) \cdot V5 \times PFC \quad 14$$

This procedure can be compared to partial correlation analysis, where the effect of the established predictors is removed from a new predictor to assess the improvement in fit.

The influence of this new variable on PP corresponds to the influence of the prefrontal cortex on the connection between V5 and PP. The interaction model is shown in Figure 5. Because our non-linear model could accommodate changes in connectivity between attention and "no attention" the entire time-series was analysed (i.e. attention specific changes are explicitly modelled).

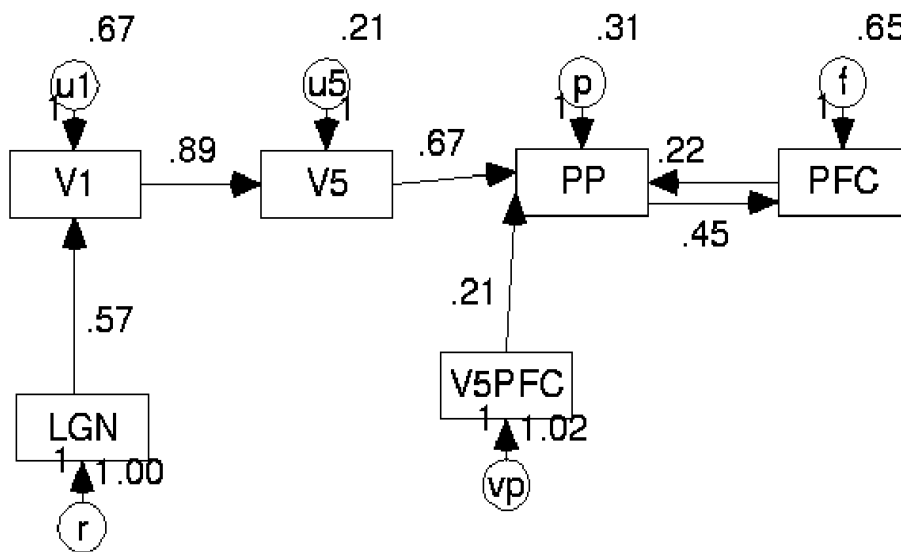


**Figure 5.** A sketch of the extended model of the dorsal visual pathway with the modulatory influence of the prefrontal cortex (PFC) on the connection between V5 and PP. The main effect of PFC is also included to show whether the interaction is significant in the presence of the main effect.

As described in the linear model, we tested for the significance of the interaction effect by comparing a restricted and free model. In the restricted model the interaction term (i.e. path from V5PFC to PP) was set to zero. It is important to note that testing for an interaction is only valid in the presence of the main effects (i.e. paths from V5 and PFC to PP). Although the path coefficient for the interaction term was only 0.21, omitting this term led to a significantly reduced model fit ( $\chi^2=34, p<0.01$ ).

The presence of an interaction effect of the PFC on the connection between V5 and PP can also be illustrated by a simple regression analysis. If PFC shows a positive modulatory influence on the path between V5 and PP, the influence of V5 on PP should depend on the activity of PFC. This can be tested, by splitting the observations into two sets, one containing observations in which PFC activity is high and another one in which PFC activity is low. It is now possible to perform separate regressions of PP on V5 for both sets. If the hypothesis of positive modulation is true, the slope of the regression of PP on V5 should be steeper under high

values of PFC. Figure 6 shows exactly this and provides the regression coefficients and the F-statistic for the difference in slope.

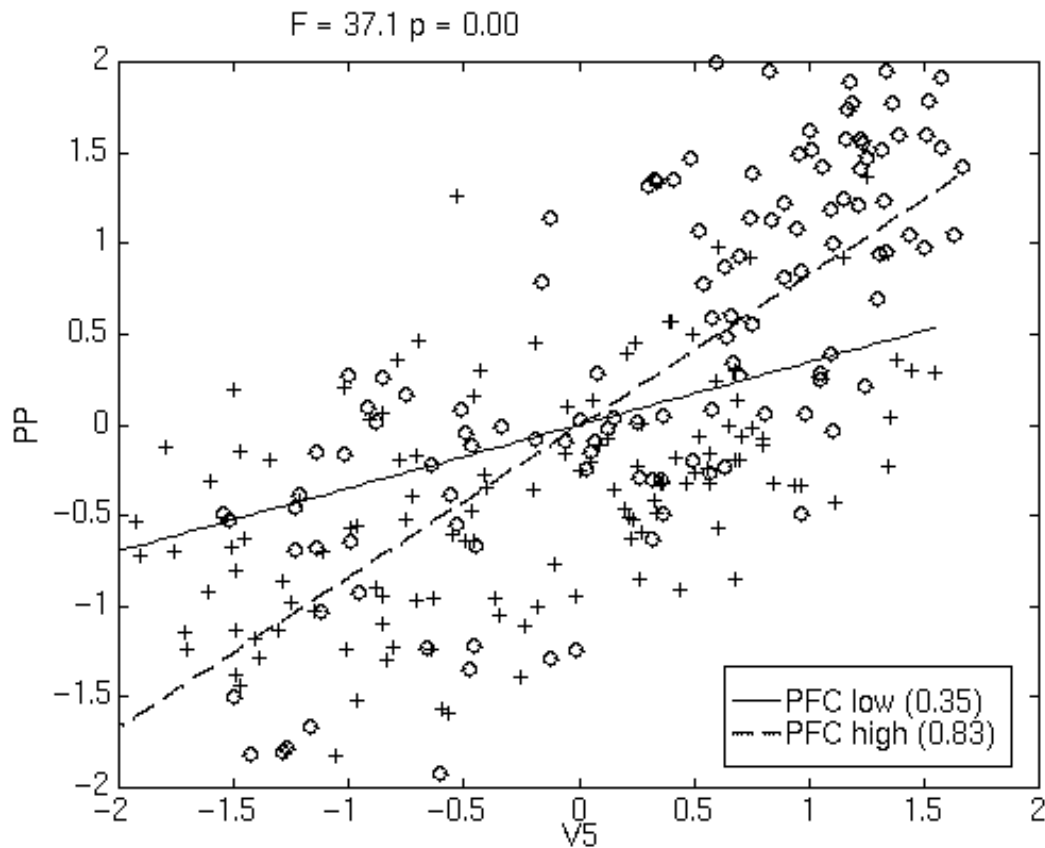


**Figure 6.** An alternative way of showing the modulatory effect of the PFC on the connection between V5 and PP. All observations were divided into two groups, one with observations in which PFC activity is high, one in which PFC activity is low. The graph shows separate regression curves for both groups and the significance for the differences in slope for the right hemisphere.

### VI.C. Connectivity vs. categorical analyses

One obvious advantage of the assessment of effective connectivity is that it allows one to test hypotheses about the integration of cortical areas. For example the categorical comparison between “attention” and “no attention” revealed prestriate, parietal and frontal activations. However the only statement possible, is that these areas show higher rCBF during the “attention” condition as opposed to the “no attention” condition. The analysis of effective connectivity revealed two additional results. Firstly, we showed, that attention predominantly affects the pathway from V5 to PP and to a lesser degree from V1 to V5. Secondly, the introduction of non-linear interaction terms allowed us to test the hypothesis about how these modulations are mediated. The latter analysis suggested that the prefrontal cortex could exert a modulatory influence on posterior cortical areas.

## VII. Regression with time-varying coefficients

As demonstrated in section III, the basic linear model can be seen as a linear regression. The regression coefficient is then interpreted as a measure of the connectivity between areas. This interpretation of course implies that this influence is mediated by neural connections with an effective strength equal to the regression coefficient. Using this approach one immediately makes the assumption that the effective connectivity does not

change over observations, because only a single regression coefficient for the whole time-series is estimated. This is unsuitable for the assessment of effective connectivity in functional imaging as the goal in some experiments is to demonstrate changes in effective connectivity, for instance as a function of different conditions (eg “attention” and “no attention”) or simply time itself. In the framework of regression analysis there are two ways around this problem: Firstly, one could split up the data in different groups according to the experimental condition (eg. “attention” and “no attention”) and then test for the difference of the regression coefficients, similar to the approach shown in Figure 6. The second, more general solution is to expand the explanatory variable in terms of a set of basis functions to account for changes in connectivity. Here we will present another alternative that allows one to characterise the variation of the regression coefficient using the framework of state-space models and the Kalman filter (Kalman, 1960).

## VII A Mathematical background

Consider the classical regression model

$$y_t = x_t' \beta + \epsilon_t \quad (15)$$

where  $x$  is a vector of explanatory variables and  $\beta$  is the vector of unknown parameters. Usually  $\beta$  is estimated as

$$\hat{\beta} = \text{pinv}(x)y \quad (16)$$

However  $\hat{\beta}$  can also be calculated recursively with the advantage that inversion of a smaller matrix is necessary. This approach is known as recursive least squares (Harvey, 1993). This basic model is now extended to allow  $\beta$  to evolve over time according to various stochastic processes, in our example a random walk. This is another major difference to the use of basis functions, since a random walk cannot be modelled by basis functions.

We will now introduce the concept of state-space models. State-space models originate from the control theory literature. Consider a satellite in its orbit. The state of the satellite (ie. absolute position and speed) are the state variables that cannot be measured directly. These variables describe the state of the system at time  $t$ . What is measured in our example is the position of the satellite relative to radio stations on the earth. We also assume that we know how the state variables evolve over time. The task now is to use the observations to make an inference about the state variables. In this context a state-space model is defined by 2 equations: the measurement and updating equation.

Coming back to the regression model with time-varying coefficients, this model can be phrased in terms of a measurement equation (17) and an updating equation (18) as well:

$$y_t = x_t' \beta_t + \epsilon_t \quad (17)$$

$$\beta_t = \beta_{t-1} + \eta_t \quad (\eta_t \sim \text{NID}(\mathbf{0}, \mathbf{Q})) \quad (18)$$

where the measurement equation is the same as the standard regression equation (15). These two equations explain the relation between the state variable  $\beta$  (which is the regression coefficient) and the observed time-series  $y$  and the explanatory variable  $x$ . The updating equation determines how  $\beta$  can change over time. In our case  $\beta$  is non-stationary and able to evolve in such a way that the model can accommodate fundamental changes in structure. The term  $\mathbf{Q}$ , the variance of the random error term  $\eta$ , determines to which extent it can vary. If  $\mathbf{Q}$  is zero the model collapses to an ordinary regression model since  $\beta_t = \beta_{t-1}$ . Note that in the multivariate case  $\mathbf{Q}$  is a variance-covariance matrix.

A recursive algorithm known as the Kalman filter can now be applied to estimate the state-variable ( $\beta$ ) at each point in time and also allows to estimate the log-likelihood function of the model. A numerical optimisation algorithm is then employed to maximize the likelihood function with respect to  $\mathbf{Q}$ . As the Kalman filter is a recursive procedure, the estimation of  $\beta_t$  is based on all observations up to time  $t$ . Therefore the filtered estimates

will be more accurate towards the end of the sample. This fact is corrected for by the Kalman smoothing algorithm which is employed post-hoc and runs backwards in time, taking account of the information made available after time  $t$ . Details of the Kalman filter and smoothing recursions can be found in standard textbooks of time-series analysis and econometrics (e.g. Chow, 1983; Harvey, 1990).

### VII B Application

Again we used data from the fMRI study looking at the effect of attention to visual motion. Structural equation modelling indicated an increase in connectivity between V5 and PP during attention. Here we use exactly the same time-series (V5 and PP) to replicate this finding using a regression with time-varying coefficients.

The model is

$$PP = V5 + \beta_t \quad (19)$$

and

$$\beta_t = \beta_{t-1} + \epsilon_t \quad (\epsilon_t \sim \text{NID}(\mathbf{0}, \mathbf{Q})) \quad (20)$$

Using the Kalman filter recursions with a Nelder-Mead simplex search optimisation,  $\mathbf{Q}$  was determined to be  $7.4e-2$ . Figure 7 shows the smoothed estimate of  $\beta_t$  varying over time. The background of the figure indicates the different conditions of the scan. It is clearly seen that  $\beta_t$  is increased during “attention” (light gray) and decreased during “no attention”.(dark gray).

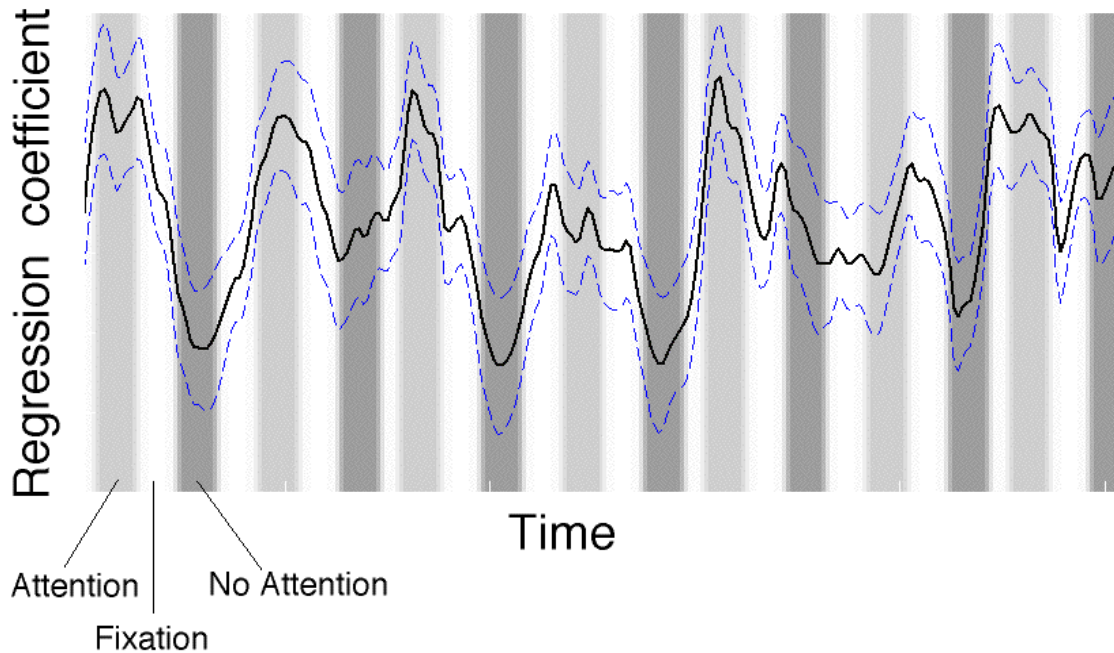


**Figure 7.** Smoothed estimators of  $\beta_t$  estimated with the Kalman filter and smoothing recursions. Note that the peaks of the coefficient curve coincides with the attention conditions. The dashed line shows the standard error of the coefficient

This method also allows statistical inference on whether parameter variation over time is significant. This is done by testing the estimated  $\mathbf{Q}$  against  $\mathbf{Q}_0$  which is set to zero in our case. This inference is based on the

likelihood statistic  $[-2(\log L(\mathbf{Q}_0) - \log L(\mathbf{Q}))]$  which is chi-squared distributed. However it should be noted that testing against  $\mathbf{Q}_0 = 0$  (no variation in the coefficient) tends to a more conservative test of the stability of  $\mathbf{Q}$ , as the distribution under the null-hypothesis is more concentrated towards the origin than a chi-squared distribution (Garbade, 1977). Besides the estimation of the state variables (ie. regression coefficient) the Kalman filter also provides the standard error for this parameter (plotted as dashed lines in Figure 7).

### VIII. Issues of validity

A major criticism of path analysis is the validity of the model. The issue of construct validity applies to most models of effective connectivity. The difficulty in proving that a model is correct does not only pertain to effective connectivity: Every discussion of functional imaging experiments trying to explain results of categorical comparisons, on the basis of connected networks, faces this problem. This debate can also be seen from a different angle: A simple subtraction paradigm in functional imaging most often reveals more than one site of activation. It is necessary to have a hypothesis about the interconnections of these regions (functional/anatomical model), to explain the integration of the (spatially remote) activations. Structural equation modelling and other techniques of effective connectivity can be seen as a 'reverse' approach, where an anatomical model is specified and can then be tested under different experimental conditions. This technique has been successfully applied for instance comparing object to spatial vision as shown in a study by McIntosh and Gonzales-Lima (1994b) and in our fMRI example.

The measurements used in all examples of this chapter were *hemodynamic* in nature. This limits an interpretation at the level of *neuronal* interactions. However the analogy between the form of the non-linear interaction between V1 and V2 activity and voltage-dependent connections is a strong one. It is possible that the modulatory impact of V2 on V1 is mediated by predominantly voltage-dependent connections. The presence of horizontal voltage-dependent connections within V1 has been established in cat striate cortex (Hirsch & Gilbert 1991). We know of no direct electrophysiological evidence to suggest that extrinsic backward V2 to V1 connections are voltage-dependent; however our results are consistent with this. An alternative explanation for modulatory effects, which does not necessarily involve voltage-dependent connections, can again be found in the work of Aertsen & Preissl (1991). Recall that they concluded effective connectivity varies strongly with, or is modulated by, pool activity. The mechanism related to the efficacy of subthreshold EPSPs in establishing dynamic interactions as a function of post-synaptic depolarisation, which in turn depends on the tonic background of activity. This clearly relates to the idea that sensitivity to afferent input increases with intrinsic activity. The original presentation of these results and a fuller discussion can be found in Friston *et al* 1995).

It is also important to clarify the terms 'excitatory' and 'inhibitory' effects in the context of effective connectivity. The conclusion that a positive path coefficient from region A to B, reflects a predominantly excitatory pathway between A and B is wrong. As mentioned before all measurements are hemodynamic in nature and one has to keep in mind that both excitation and inhibition can lead to an increase in regional cerebral blood flow.

This chapter has reviewed some basic concepts of effective connectivity in neuroimaging. Methods currently used to assess effective connectivity have been demonstrated. The first example demonstrated that non-linear interactions can be characterised using simple extensions of linear models. In the second example structural equation modelling was introduced as a device which allows one to combine observed changes in cortical activity and anatomical models. Both examples concentrated on changes in effective connectivity and allowed a comprehensive description of the interacting areas of the network on a functional level. Although less than a mature field the approach to neuroimaging data and regional interactions discussed here and elsewhere is an exciting endeavour that is starting to attract more and more attention.

### References

Aertsen A & Preissl H (1991) Dynamics of activity and connectivity in physiological neuronal Networks in Non Linear Dynamics and Neuronal Networks Ed Schuster HG VCH publishers Inc., New York NY USA p281-302

- Assad JA, Maunsell JH (1995) *Neuronal correlates of inferred motion in primate posterior parietal cortex*. Nature, **373**, 518-21.
- Binmore KG (1982) **Mathematical analysis** (2nd Ed) Cambridge University Press. Cambridge p218
- Bollen KA (1989) **Structural Equations with Latent Variables** John Wiley & Sons. New York
- Chatfield C (1989) **The Analysis of Time Series - An introduction** Chapman and Hall. London
- Chatfield C, Collins AJ (1995) **Introduction to multivariate analysis** Chapman and Hall London
- Chow GC (1983) **Econometrics**. New York: McGraw Hill.
- Corbetta M, Miezin FM, Dobmeyer S, Shulman GL, Petersen SE (1991) *Selective and divided attention during visual discrimination of shape, color, and speed: Functional anatomy by positron emission tomography*. Journal of Neuroscience **13**:1202-1226
- Friston KJ Frith CD Liddle PF & Frackowiak RSJ (1993a) *Functional connectivity: The principal component analysis of large (PET) data sets*. J. Cereb. Blood Flow Metab. **13**:5-14
- Friston KJ Frith CD & Frackowiak RSJ (1993b) *Time-dependent changes in effective connectivity measured with PET*. Human Brain Mapping **1**:69-80
- Friston KJ, Ungerleider LG, Jezzard P and Turner R (1995) *Characterizing modulatory interactions between V1 and V2 in human cortex with fMRI*. Human Brain Mapping **2**:211-224
- Garbade K (1977) *Two methods for examining the stability of regression coefficients*. Journal of the American Statistical Association, **72**, 54-63.
- Gerstein GL & Perkel DH (1969) *Simultaneously recorded trains of action potentials: Analysis and functional interpretation* Science **164**:828-830
- Gerstein GL, Bedenbaugh P & Aertsen AMHJ (1989) *Neuronal assemblies* IEEE Trans. on Biomed. Engineering **36**:4-14
- Girard P & Bullier J (1988) *Visual activity in area V2 during reversible inactivation of area 17 in the macaque monkey*. J Neurophysiol. **62**:1287-1301
- Gochin PM, Miller EK, Gross CG & Gerstein GL (1991) *Functional interactions among neurons in inferior temporal cortex of the awake macaque* Exp. Brain Res. **84**:505-516
- Golub GH & Van Loan CF (1991) **Matrix computations** (2nd ed) The Johns Hopkins University Press, Baltimore and London. p241-248
- Haberly LB (1991) *Olfactory cortex*. in **The synaptic organization of the brain**. ed. Shepard GM. Oxford University Press, Oxford p331
- Harvey AC (1990) **Forecasting, structural time series models and the Kalman filter**. Cambridge: Cambridge University Press.
- Harvey AC (1993) **Time Series Models**. London: Harvester & Wheatsheaf.
- Hirsch JA & Gilbert CD (1991) *Synaptic physiology of horizontal connections in the cat's visual cortex*. J. Neurosci **11**:1800-1809
- Horwitz B, McIntosh AR, Haxby JV, Kurkjian M, Salerno JA, Schapiro MB et al. (1995) *Altered brain functional interactions during visual processing in Alzheimer type dementia*. NeuroReport, **6**, 2287-2292.
- Horwitz B, Sporns O (1994) *Neural modeling and functional neuroimaging*. Human Brain Mapping, **1**, 269-283.
- Kalman RE (1960) *A new approach to linear filtering and prediction problems*. Transactions ASME Journal of Basic Engineering, **D 82**, 35-45.
- Kenny DA, Judd CM (1984) *Estimating nonlinear and interactive effects of latent variables*. Psychol Bull **96**:201-210
- Lagreze HL, Hartmann A Anzinger G, Shaub A and Deister A (1993) *Functional cortical interaction patterns in visual perception and visuospatial problem solving*. J. Neurolog Sci. **114**:25-35

- Lawler KA, Cowey A (1987) *On the role of posterior parietal and prefrontal cortex in visuo-spatial perception and attention*. *Exp Brain Res*, **65**, 695-8.
- McIntosh AR & Gonzalez-Lima F (1991) *Structural modelling of functional neural pathways mapped with 2-deoxyglucose: Effects of acoustic startle habituation on the auditory system*. *Brain Res* **547**:295-302
- McIntosh AR, Grady CL, Ungerleider LG, Haxby JV, Rapoport SI and Horwitz B (1994a) *Network analysis of cortical visual pathways mapped with PET*. *J Neurosci* **14**:655-666
- McIntosh AR & Gonzalez-Lima F (1994b) *Structural equation modelling and its application to network analysis in functional brain imaging*. *Human Brain Mapping* **2**:2-22
- Mesulam MM (1990) *Large-scale neurocognitive networks and distributed processing for attention, language, and memory*. *Ann-Neurol*, **28**, 597-613.
- Mishkin M, Ungerleider LG, Macko KA (1983) *Object vision and spatial vision: two cortical pathways*. *Trends Neurosci*, **6**, 414-17.
- O'Craven KM, Savoy RL (1995) *Voluntary attention can modulate fMRI activity in human MT/MST*. *Invest. Ophthalmol. Vis. Sci. (suppl.)*, **36**, S856.
- Palus M, Dvorak I & David I (1991) *Remarks on spatial and temporal dynamics of EEG*. In Dvorak I & Holden AV (eds.) **Mathematical approaches to brain imaging diagnostics**. Manchester University Press:Manchester and New York p369-385
- Sandell JH & Schiller PH (1982) *Effect of cooling area 18 on striate cortex cells in the squirrel monkey* *J. Neurophysiol.* **48**:38-38
- Schiller PH & Malpeli JG (1977) *The effect of striate cortex cooling on area 18 cells in the monkey* *Brain Res.* **126**:366-369
- Talairach P & Tournoux J (1988) **A Stereotactic coplanar atlas of the human brain**. Stuttgart:Thieme
- Treue S, Maunsell HR (1996) *Attentional modulation of visual motion processing in cortical areas MT and MST*. *Nature*, **382**, 539-41.
- Tsonis AA (1992) *Chaos: From theory to applications*, Plenum Press: New York and London p221